brane stalks (Fig. 4A). Moreover, the trimers are open, as would be predicted if the stalks undergo homomeric interactions.

Here we show that homo-oligomerization has important functional consequences as well. Two different Asn mutations, separated by 10 Å along the β3 transmembrane helix, induced homo-oligomerization in vitro and constitutive integrin activation and clustering in vivo. We have also considered the possibility that the M701N and G708N mutations help activate the integrin by disrupting a heterodimeric association between the αIIb and β3 transmembrane helices in the inactive state of the integrin. However, we find this possibility unlikely. Recently reported nuclear magnetic resonance structural data indicate that the αIIb and β3 cytoplasmic tails are able to physically interact (*10*). However, extrapolation of the transmembrane helices from this structure (*10*) shows that they are too far apart to allow interhelical contacts involving residues 701 and 708. On the basis of this model and others, the α and β transmembrane helices are proposed to interact (*28*, *29*). However, several of the Asn mutants that might have been expected to affect heterodimerization had no effect on αIIbβ3 activity.

αIIbβ3 in platelets exists in either of two affinity states whose relative proportion is determined by platelet stimulation (*30*). Here, we have demonstrated that the equilibrium between these states can be shifted by enhancing the tendency of the β3 transmembrane domain to undergo homo-oligomerization. Thus, the transmembrane helix-cytoplasmic domain of β3 is appropriately poised to allow dynamic changes in the αIIbβ3 activation state. Moreover, interactions that occur only in the activated state would be expected to stabilize this conformation of αIIbβ3. Thus, homo-oligomerization provides a mechanism for driving the equilibrium toward an activated state, while simultaneously inducing the formation of αIIbβ3 clusters (Fig. 4B). Additional interactions involving the αIIb and/or β3 cytoplasmic domains could finely modulate the overall activation process.

References and Notes

1. R. C. Liddington, M. H. Ginsberg, *J. Cell Biol.* **158**, 833 (2002).
2. R. O. Hynes, *Cell* **110**, 673 (2002).
3. J. W. Weisel, C. Nagaswami, G. Vilaire, J. S. Bennett, *J. Biol. Chem.* **267**, 16637 (1992).
4. M. V. Nermut, N. M. Green, P. Eason, S. S. Yamada, K. M. Yamada, *EMBO J.* **7**, 4093 (1988).
5. J.-P. Xiong *et al.*, *Science* **294**, 339 (2001).
6. J. Takagi, B. M. Petre, T. Walz, T. A. Springer, *Cell* **110**, 599 (2002).
7. M. A. Arnaout, S. L. Goodman, J. P. Xiong, *Curr. Opin. Cell Biol.* **14**, 641 (2002).
8. M. J. Calzada, M. V. Alvarez, J. González-Rodríguez, *J. Biol. Chem.* **277**, 39899 (2002).
9. J. Takagi, H. P. Erickson, T. A. Springer, *Nature Struct. Biol.* **8**, 412 (2001).
10. O. Vinogradova *et al.*, *Cell* **110**, 587 (2002).
11. R. Li *et al.*, *Proc. Natl. Acad. Sci. U.S.A.* **98**, 12462 (2001).
12. F. X. Zhou, H. J. Merianos, A. T. Brunger, D. M. Engelman, *Proc. Natl. Acad. Sci. U.S.A.* **98**, 2250 (2001).
13. H. Gratkowski, J. D. Lear, W. F. DeGrado, *Proc. Natl. Acad. Sci. U.S.A.* **98**, 880 (2001).
14. R. B. Basani *et al.*, *J. Biol. Chem.* **276**, 13975 (2001).
15. Materials and Methods are available as supporting online material at *Science* Online.
16. Single-letter abbreviations for the amino acid residues are as follows: A, Ala; C, Cys; D, Asp; E, Glu; F, Phe; G, Gly; H, His; I, Ile; K, Lys; L, Leu; M, Met; N, Asn; P, Pro; Q, Gln; R, Arg; S, Ser; T, Thr; V, Val; W, Trp; and Y, Tyr.
17. J. S. Bennett, G. Vilaire, *J. Clin. Invest.* **64**, 1393 (1979).
18. T. K. Gartner, J. S. Bennett, *J. Biol. Chem.* **260**, 11891 (1985).
19. J. S. Bennett, J. A. Hoxie, S. F. Leitman, G. Vilaire, D. B. Cines, *Proc. Natl. Acad. Sci. U.S.A.* **80**, 2417 (1983).
20. J. S. Bennett *et al.*, *Blood* **97**, 3093 (2001).
21. S. J. Shattil, J. A. Hoxie, M. Cunningham, L. F. Brass, *J. Biol. Chem.* **260**, 11107 (1985).
22. R. Li *et al.*, data not shown.
23. F. G. Giancotti, E. Ruoslahti, *Science* **285**, 1028 (1999).
24. M. E. Lukashev, D. Sheppard, R. Pytela, *J. Biol. Chem.* **269**, 18311 (1994).
25. S. J. Shattil, L. F. Brass, J. S. Bennett, P. Pandhi, *Blood* **66**, 92 (1985).
26. L. A. Fitzgerald, D. R. Phillips, *J. Biol. Chem.* **260**, 11366 (1985).
27. R. R. Hantgan *et al.*, *J. Biol. Chem.* **278**, 3417 (2003).
28. K. E. Gottschalk, P. D. Adams, A. T. Brunger, H. Kessler, *Protein Sci.* **11**, 1800 (2002).
29. B. D. Adair, M. Yeager, *Proc. Natl. Acad. Sci. U.S.A.* **99**, 14059 (2002).
30. R. Litvinov, H. Shuman, J. S. Bennett, J. W. Weisel, *Proc. Natl. Acad. Sci. U.S.A.* **99**, 7426 (2002).
31. C. Choma, H. Gratkowski, J. D. Lear, W. F. DeGrado, *Nature Struct. Biol.* **7**, 161 (2000).
32. N. Beglova, S. C. Blacklow, J. Takagi, T. A. Springer, *Nature Struct. Biol.* **9**, 282 (2002).

33. We thank C. S. Abrams for advice on FAK phosphorylation, and Mary A. Leonard for assistance on Fig. 4B. R.L. was supported by a postdoctoral fellowship from the Cancer Research Fund of the Damon Runyon-Walter Winchell Foundation. Supported by NIH grants HL40387 and HL54500 to J.S.B. and W.F.D.

Supporting Online Material

www.sciencemag.org/cgi/content/full/300/5620/795/DC1
Materials and Methods
Figs. S1 and S2
References

15 October 2002; accepted 21 March 2003

Closing of the Nucleotide Pocket of Kinesin-Family Motors upon Binding to Microtubules

Nariman Naber,[1]* Todd J. Minehardt,[5]† Sarah Rice,[2] Xiaoru Chen,[6] Jean Grammer,[6] Marija Matuska,[1] Ronald D. Vale,[2] Peter A. Kollman,[3]‡ Roberto Car,[5] Ralph G. Yount,[6,7] Roger Cooke,[1,4] Edward Pate[8]

We have used adenosine diphosphate analogs containing electron paramagnetic resonance (EPR) spin moieties and EPR spectroscopy to show that the nucleotide-binding site of kinesin-family motors closes when the motor•diphosphate complex binds to microtubules. Structural analyses demonstrate that a domain movement in the switch 1 region at the nucleotide site, homologous to domain movements in the switch 1 region in the G proteins [heterotrimeric guanine nucleotide–binding proteins], explains the EPR data. The switch movement primes the motor both for the free energy–yielding nucleotide hydrolysis reaction and for subsequent conformational changes that are crucial for the generation of force and directed motion along the microtubule.

The generation of motion by kinesin-family motor proteins results from a carefully choreographed interaction involving the motor itself, hydrolysis of the triphosphate substrate, adenosine triphosphate (ATP), and interaction with the microtubule (MT) roadway upon which directed translocation occurs. The conformational changes in the kinesin motor that link the free energy–yielding hydrolysis reaction to motility remain unresolved. A currently popular hypothesis draws on structural homologies observed in structures of the evolutionarily related (*1*, *2*) G proteins and myosin. According to this hypothesis, nucleotide-induced conformational changes in the switch 1 and switch 2 regions at the nucleotide-binding site in kinesin-family motors are modulated by MT interactions and propagated to the distant neck region that functions as the motion-transducing element, re-

[1]Department of Biochemistry, [2]Department of Cellular and Molecular Pharmacology, [3]Department of Pharmaceutical Chemistry, [4]Cardiovascular Research Institute, University of California, San Francisco, CA 94143, USA. [5]Department of Chemistry, Princeton University, Princeton, NJ 08544, USA. [6]School of Molecular Biosciences, [7]Department of Chemistry, [8]Department of Mathematics, Washington State University, Pullman, WA 99164, USA.

*To whom correspondence should be addressed. E-mail: naber@itsa.ucsf.edu
†Present address: Department of Chemistry, University of Colorado, Denver, CO 80217, USA.
‡Deceased.

viewed in (*2*–*7*). In order to establish this, or competing hypotheses, the structural and biochemical links between nucleotide hydrolysis and motion must be identified in kinesin-family motors. EPR spectroscopy is a powerful tool for monitoring conformational changes in proteins (*8*, *9*). Here we use nucleotide analogs containing EPR spin labels to place reporter groups at the nucleotide site of kinesin-family motors. We demonstrate an unanticipated domain movement in kinesin-family motors: the nucleotide-binding site closes when the motor binds to MTs. We relate this to a conformational change in switch 1 previously identified in the G proteins.

The nucleotide-analog spin labels used (Fig. 1A) contain an unpaired electron associated with the spin-ring nitroxide bond. When bound at the nucleotide site, thermal fluctuations result in the spin label undergoing motion in a spatial region defined by the adjacent protein surface. In a magnetic field, the resulting EPR spectrum is a highly sensitive measure of the region accessible to the probe. In Fig. 1B, this is shown in the spectra of SSL-NANDP and motor protein, ncd (*10*). Five peaks (P1 to P5) in the EPR spectra are relevant. The three central, truncated peaks, P2 to P4, arise from unbound spin label that is tumbling freely in solution (*11*). The more restricted mobility of the probe after binding to the ncd nucleotide site results in a broadening of the spectrum of ncd•SSL-NANDP (red), resulting in the introduction of a low-field peak, P1, and a high-field dip, P5. The magnitude of the low-field to high-field splitting increases with decreasing spatial mobility imposed by a more restrictive protein surface (*12*). The P1-P5 splitting from spin label in the MT•ncd•SSL-NANDP state (blue) increased relative to that in the ncd•SSL-NANDP state, consistent with a closing of the ncd nucleotide-binding site upon binding to MTs. In the presence of MTs, P1-P5 spectral broadenings are observed for all five probes in Fig. 1A and for both ncd and kinesin (Table 1). In some experiments, the P1 component was visible only as a low-field shoulder on the larger P2 component (Fig. 1C; fig. S1) so that only a lower bound for the increase in the P1-P5 splitting could be determined. Hydrolysis rates were comparable to that of ATP for all triphosphate spin labels (table S1) implying catalytically competent binding at the nucleotide site and confirming that our observations are on the diphosphate species. The decrease in mobility is not simply the trivial result of motor immobilization upon binding to the MTs because the P1-P5 splittings for both kinesin•SSL-NANDP [6.00 ± 0.05 mT, 4 observations (obs.)] and ncd•SSL-NANDP (5.87 ± 0.05 mT, 5 obs.) immobilized on sulfopropyl (SP) or carboxymethyl (CM) sepharose beads were not statistically different from values for the free proteins.

Thus two kinesin-family motors, one with plus-end directed MT motion (kinesin) and the other with minus-end directed motion (ncd); three nucleotide diphosphate spin label analogs; and two non-nucleoside diphosphate analogs consistently show a decrease in mobility upon binding to MTs. This supports the notion that this is not a special case arising from a single spin label or a single motor protein. Because the primary restriction on mobility is provided by steric interference of the protein surface near the probe, we conclude that the nucleotide-binding site closes upon binding to MTs. Assuming the probe is constrained to move within a cone, the changes in mobility can be modeled as alterations

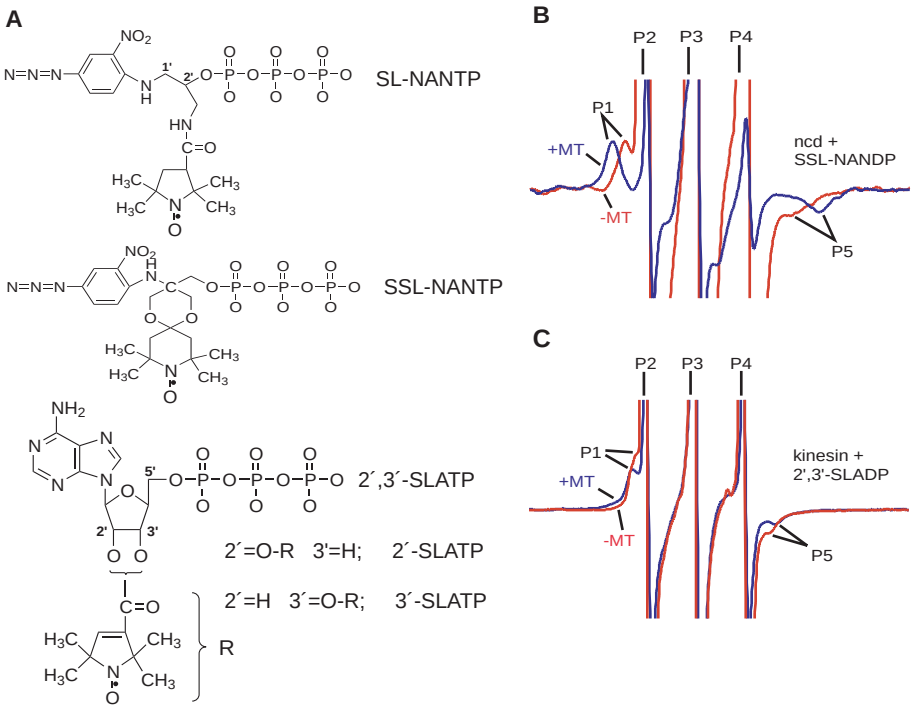

Fig. 1. (**A**) The ATP analogs used in these studies. The horizontal structure in the top two panels (a substituted phenyl ring–amino ethyl spacer–triphosphate structure) is NANTP, from which SSL-NANTP and SL-NANTP are derived. The SLATP structures are derived from adenosine triphosphate via ribose modifications. (**B**) EPR spectra of SSL-NANDP bound to ncd in the presence (blue) and absence (red) of MTs. (**C**) Spectra of 2′, 3′-SLADP bound to kinesin, with peak P1 obscured by P2. The heavy arrow shows the point taken as the lower bound for P1-P5 splitting determination. A 2:1 analog:motor ratio was used in the experimental buffer (*10*).

Table 1. Summary of the high- to low-field probe splittings and cone angles of mobility for ncd and kinesin. The P1-P5 splitting for nucleotide-analog EPR probes bound to two kinesin-family motors in the absence and presence of MTs are given. The experimentally determined effective cone angles for probe mobility in the absence and presence of MTs are given as mean ± SEM (number of observations); the effective cone angles of mobility as modeled by molecular dynamics for ncd are given in square brackets. The experimentally determined decrease in cone angle upon binding to microtubules is given, and the modeled decrease in mobility angle based upon the switch 1–open to –closed transition in ncd is also given.

Analog	Splitting (mT)		Cone angle (°)		Δ Angle (°)	
	−MT	+MT	−MT	+MT	EPR	Model
ncd						
SSL-NANDP	5.84 ± 0.04 (7)	6.86 ± 0.02 (7)	84 [100]	40 [50]	44	50
SL-NANDP	<6.15 ± 0.01 (2)	6.76 ± 0.07 (2)	>72 [90]	44 [50]	>28	40
2′-SLADP	5.40 ± 0.03 (4)	5.76 ± 0.02 (4)	98 [100]	86 [90]	12	10
3′-SLADP	<4.26 ± 0.03 (4)	4.69 ± 0.02 (4)	>134 [130]	122 [110]	>12	20
2′, 3′-SLADP	<4.78 ± 0.03 (4)	5.30 ± 0.05 (5)	>118	102	>16	
kinesin						
SSL-NANDP	5.94 ± 0.03 (10)	6.80 ± 0.06 (6)	79	44	35	
SL-NANDP	5.60 ± 0.01 (2)	6.47 ± 0.08 (3)	92	60	32	
2′-SLADP	<4.64 ± 0.01 (3)	4.95 ± 0.01 (3)	>122	112	>10	
3′-SLADP	4.31 ± 0.02 (4)	4.59 ± 0.04 (4)	134	123	11	
2′, 3′-SLADP	<4.56 ± 0.04 (3)	5.11 ± 0.02 (2)	>126	108	>18	

in the vertex angle (*12*). Effective cone angles are given in Table 1.

A given probe reports a similar change in mobility when either kinesin•analog or ncd•analog binds to MTs. However, different probes yield quite disparate MT-dependent cone angle changes, arguing that the closing of the nucleotide pocket is not spatially uniform. This difference is particularly evident when comparing the results from SL-NANDP to the results with the three ribose-modified probes (Fig. 1A). All contain the same carbonyl linkage to the spin moiety, but only SL-NANDP shows substantial restriction of motion upon binding to MTs. Thus localized conformational changes at the nucleotide site are required to explain the data.

X-ray crystallography has shown that the conformations of the switch 1 and switch 2 regions at the nucleotide site of the more extensively studied G proteins change in response to the bound nucleotide, transmitting information to the periphery of the proteins. In turn, the binding of other regulatory proteins can change the conformation of the switch regions, affecting the rates of hydrolysis (*7*). By structural homology, switch 2 has been hypothesized to play a role in the connection between the nucleotide and the peripheral, force-transducing elements in both the kinesin-family and myosin motor proteins. The role of switch 1 in the motor proteins has remained obscure, however, and we address this issue below.

X-ray structures of kinesin-family motors have shown switch 1 to be displaced well away from the nucleotide, with a very open triphosphate-binding domain (*13*–*21*). Both an intermediate conformation of kinesin-family motors with switch 1 partly closing the triphosphate-binding domain (*18*) and a disordered switch 1 domain (*21*) have been identified. In contrast to kinesin, the switch 1 region in all myosin x-ray structures is found adjacent to the nucleotide, forming in conjunction with switch 2 and the P-loop, a closed "phosphate tube" (*22*) in which the triphosphates are tightly bound. However, biochemical and biomechanical evidence demonstrates that this closed conformation of the phosphate tube must open during the motor cycle (*23*). We shall refer to conformations of switch 1 adjacent to, and displaced from, the nucleotide as the switch 1–closed and the switch 1–open conformations, respectively. Further support of the flexibility of switch 1 comes from G protein structures where switch 1 is seen in both closed (*24*) and open (*25*) positions. These observations all suggest that the switch 1 region can undergo a major conformational change. Indeed, a completely closed triphosphate-binding domain, with switch 1 forming a closed phosphate tube identical to that seen in myosin (switch 1–closed), has also been shown to be a thermodynamically stable conformation of the nucleotide site in kinesin-family motors (*26*).

All kinesin-family x-ray structures have been determined in the absence of MTs. However, EPR studies using a probe covalently attached at the switch 1 region of kinesin have previously shown that there is a conformational change in the switch 1 region when the motor binds to MTs (*27*). Given that there is a MT-dependent conformational change in switch 1 and a nonuniform closing of the nucleotide-binding site upon binding to MTs, we can ask the degree to which a switch 1 displacement could be implicated in the nonuniform closing.

Kinesin and ncd have similar active sites (*13*, *14*), and using the myosin- and kinesin-family structural homologies and molecular graphics visualization, the nucleotide EPR probes were docked at the active site of ncd (*28*). 3′-SLADP docked into the switch 1–open (*14*) and switch 1–closed (*26*) conformers is shown in Fig. 2, A and B, respectively. The switch 1–closed conformation reduces the spatial region available for probe motion, with magnitude related to the degree with which the probe interacts with the switch 1–closed conformer. In the ncd•3′-SLADP structure, the spin moiety projects out into the solvent from the ribose ring, and little interaction of switch 1 with the spin ring is anticipated in even the closed conformer. The region around the spin ring remains so open that the α-phosphate is even visible in the phosphate tube (Fig. 2B). Molecular dynamics (MD) simulations were used to provide a more quantitative estimate of probe mobility. As anticipated, the MD-modeled cone angle of mobility decreased from 130° to only 110° in the switch 1–open to switch 1–closed transition (Table 1). Ncd•2′-SLADP showed a comparable geometry and cone angles. In contrast, the spin ring of SL-NANDP at the closed active site (Fig. 2C) is attached at C2′ of NANTP (Fig. 1A), which by structural analogy with myosin NANTP-based structures corresponds to the C5′ position of ADP (Fig. 1A) (*28*). The spin-ring moiety does not extend as far out into the solvent domain as with the ribose-modified SL-ADP analogs, and severe hindrance of probe mobility in the switch 1–closed conformer is now anticipated. MD yielded an effective mobility angle of the spin label of only 50° in the switch 1–closed conformer. With SSL-NANDP docked at the nucleotide site in the closed conformer (Fig. 2D), both steric hindrance from switch 1 and decreased probe mobility arising from the spiro-ring structure of the probe are present. The MD-modeled motility angle decreased from 100° to 50°. MD-modeled cone angles and angle changes are summarized in Table 1. While the MD simulations with the switch 1–closed structure provided quite good agreement with the experimentally observed cone angles and cone angle changes in the spin labels, MD simulation using the partially closed switch 1 conformation of kif1a (*18*) with SSL-NANDP at the nucleotide site gave an angular distribution greater than twice that experimentally observed and, thus, cannot explain the data. Hence the EPR evidence points to a complete as opposed to a partial closing of switch 1 upon binding to MTs.

We propose a model that relates conformational changes in switch 1 to nucleotide hydrolysis and the motility cycle. Directed motion occurs when detached kinesin-family motors bind to MTs and hydrolyze ATP. Hydrolysis is thought to occur via an in-line water attack on the γ-phosphate position. The x-ray structures of myosin and the G proteins suggest that hy-

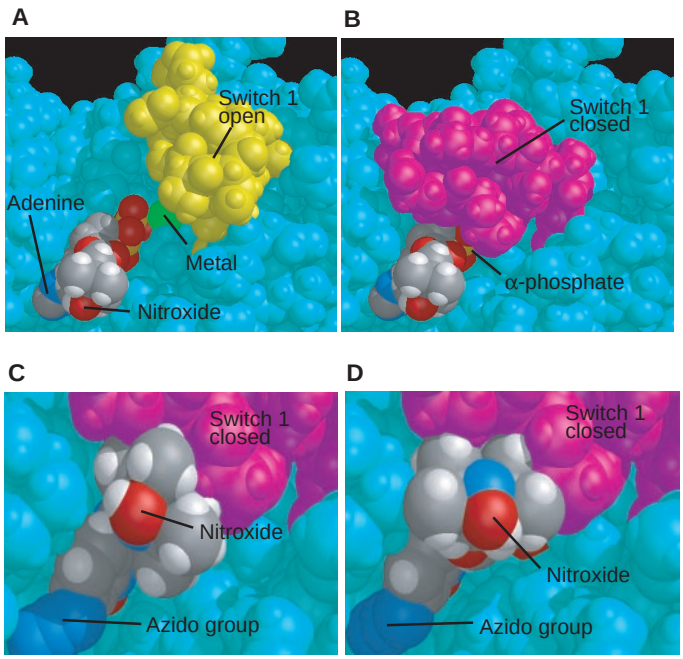

Fig. 2. Space filling model of 3′-SLADP bound to ncd in the (**A**) switch 1–open and (**B**) switch 1–closed conformations. (**C**) SL-NANDP and (**D**) SSL-NANDP bound to ncd in the switch 1–closed conformation. All views are from the same point in space. Colors are as follows: ncd is in cyan except for switch 1 (amino acids 539–554), which is yellow in the open conformer but magenta in the closed conformer; nucleotides are in the standard colors, except that phosphorus is orange and magnesium is green.

drolysis occurs when switch 1 is in a closed position, whereas thermodynamic analyses show that in kinesin motors, the closed conformation is better able to control the physical position of both the nucleotide γ-phosphate and the catalytic water for hydrolysis than is the open conformation (*26*). Thus a closing of switch 1 on binding to MTs would provide a structural rationale for the observation that the hydrolysis step in kinesin is accelerated by one to two orders of magnitude when the motor is bound to MTs (*29*). Additionally, by structural homology with myosin and the G proteins, the transmission link between the nucleotide site and the kinesin neck, which functions as the motion-transducing element, has been widely postulated to be a displacement of switch 2 via the formation of a direct hydrogen bond between a switch 2-glycine (universally conserved throughout the G protein superfamily) and a γ-phosphate oxygen of the nucleotide triphosphate (*3*, *5*, *6*). In all switch 1–open, or partially open, kinesin-family x-ray structures (*13–21*), the switch 2-glycine is instead hydrogen bonded to a conserved serine in switch 1. However, an open-to-closed displacement of switch 1 has previously been shown to disrupt the serine-glycine interaction, allowing for both the formation of the glycine-nucleotide hydrogen bond and the subsequent displacement of switch 2 (*26*). Thus, we propose that the closing of switch 1 upon binding to MTs primes the motor both for nucleotide hydrolysis and for the conformational change in switch 2 that is obligatory for directed motion to occur.

In summary, EPR spectroscopy demonstrates a direct line of communication between the MT- and the nucleotide-binding sites in kinesin-family motors, with the result that the nucleotide-binding site closes upon binding to MTs. Spectroscopic data have previously shown a conformational change in switch 1 when the motor•ADP state binds to MTs (*27*). Here, we have additionally shown that the diverse, experimentally observed changes in nucleotide analog probe mobility are readily explained by a switch 1–closed conformation in the MT-bound state that is homologous to a conformation seen in x-ray structures of myosin and the G protein superfamily, but presumably not yet captured in x-ray structures of kinesin-family motors.

References and Notes

1. F. J. Kull, R. D. Vale, R. J. Fletterick, *J. Muscle Res. Cell Motil.* **19**, 877 (1998).
2. R. D. Vale, *J. Cell Biol.* **135**, 291 (1996).
3. S. Sack, F. J. Kull, E. Mandelkow, *Eur. J. Biochem.* **262**, 1 (1999).
4. W. R. Schief, J. Howard, *Curr. Opin. Cell Biol.* **13**, 19 (2001).
5. E. P. Sablin, R. F. Fletterick, *Curr. Opin. Struct. Biol.* **11**, 716 (2001).
6. F. J. Kull, S. A. Endow, *J. Cell Sci.* **115**, 15 (2002).
7. S. R. Sprang, *Curr. Opin. Struct. Biol.* **7**, 849 (1997).
8. W. L. Hubbell, H. S. McHaourab, C. Altenbach, M. A. Lietzow, *Structure* **4**, 779 (1996).
9. D. D. Thomas, *Annu. Rev. Physiol.* **49**, 691 (1987).
10. Materials and methods are available as supporting material on *Science* Online.
11. M. S. Crowder, R. Cooke, *Biophys. J.* **51**, 323 (1987).
12. O. H. Griffith, P. C. Jost, in *Spin Labeling Theory and Applications*, L. J. Berliner, Ed. (Academic Press, NY, 1976), pp. 454–523.
13. F. J. Kull, E. P. Sablin, R. Lau, R. J. Fletterick, R. D. Vale, *Nature* **380**, 550 (1996).
14. E. P. Sablin, F. J. Kull, R. Cooke, R. D. Vale, R. J. Fletterick, *Nature* **380**, 555 (1996).
15. F. Kozielski *et al.*, *Cell* **7**, 1407 (1997).
16. S. Sack *et al.*, *Biochemistry* **36**, 16155 (1997).
17. A. M. Gulick, H. Song, S. A. Endow, I. Rayment, *Biochemistry* **37**, 1769 (1998).
18. M. Kikkawa *et al.*, *Nature* **411**, 439 (2001).
19. Y. H. Song *et al.*, *EMBO J.* **20**, 6213 (2001).
20. J. Turner *et al.*, *J. Biol. Chem.* **276**, 25496 (2001).
21. M. Yun, X. Zhang, C. G. Park, H. W. Park, S. A. Endow, *EMBO J.* **20**, 2611 (2001).
22. R. G. Yount, D. Lawson, I. Rayment, *Biophys. J.* **68**, 44S (1995).
23. E. Pate, N. Naber, M. Matuska, K. Franks-Skiba, R. Cooke, *Biochemistry* **36**, 12155 (1997).
24. D. E. Coleman *et al.*, *Science* **265**, 1405 (1994).
25. J. Goldberg, *Cell* **95**, 237 (1998).
26. T. J. Minehardt, R. Cooke, E. Pate, P. A. Kollman, *Biophys. J.* **80**, 1151 (2001).
27. N. Naber *et al.*, *Biophys. J.* **84**, 3190 (2003).
28. Coordinates have been deposited in the Protein Data Bank (1OZX). They may also be obtained from the authors.
29. Y. Z. Ma, E. W. Taylor, *J. Biol. Chem.* **272**, 717 (1997).

30. This work was supported by NIH grants AR39643 (E.P.), AR42895 (R.C., R.D.V.), DK05915 (R.G.Y.), and GM29072 (P.A.K.). T.J.M. was a Princeton University Council on Science and Technology Postdoctoral Fellow. Molecular visualizations were done using the UCSF Computer Graphics Laboratory, supported by NIH grant RR1081 to T. Ferrin.

Supporting Online Material

www.sciencemag.org/cgi/content/full/300/5620/798/DC1
Materials and Methods
Fig. S1
Table S1

14 January 2003; accepted 2 April 2003

Cooperation Between RNA Polymerase Molecules in Transcription Elongation

Vitaly Epshtein and Evgeny Nudler*

Transcription elongation is responsible for rapid synthesis of RNA chains of thousands of nucleotides in vivo. In contrast, a single round of transcription performed in vitro is frequently interrupted by pauses and arrests that drastically reduce the elongation rate and the yield of the full-length transcript. Here we demonstrate that most transcriptional delays disappear if more than one RNA polymerase (RNAP) molecule initiates from the same promoter. Anti-arrest and anti-pause effects of trailing RNAP are due to forward translocation of leading (backtracked) complexes. Such cooperation between RNAP molecules links the rate of elongation to the rate of initiation and explains why elongation is still fast and processive in vivo even without anti-arrest factors.

A high rate of transcription elongation [more than 20 nucleotides (nt) per second] in bacteria and eukaryotic cells (*1–3*) occurs despite the presence of numerous potential intrinsic and extrinsic blocks. In vitro, the majority of these blocks (pauses and arrests) are caused by backtracking of RNAP, i.e., reverse sliding of the elongation complex (EC) for one or more nucleotides along DNA and RNA (*4–6*). During backtracking, the catalytic site of RNAP loses the 3′ end of the transcript and EC becomes inactivated. Reactivation of EC in vitro either occurs spontaneously because of the reversibility of backtracking (*5*, *6*) or requires specialized factors. One class of these factors induces internal transcript cleavage by RNAP to generate the new 3′ end in the catalytic site. GreA, GreB, and TFIIS are bacterial and eukaryotic members of this group of factors, respectively (*7*, *8*). Another protein from *Escherichia coli*, Mfd, has been recently shown to use adenosine triphosphate (ATP) hydrolysis to reactivate arrested EC without transcript cleavage (*9*). Remarkably, neither GreA, GreB, TFIIS, nor Mfd are essential for cell growth under normal conditions (*10–12*), suggesting that more general mechanism(s) must be responsible for efficient transcription elongation in vivo.

In contrast to initiation, when only one RNAP molecule occupies a promoter at a time, the elongation phase can involve multiple RNAP molecules moving one after another along the same DNA molecule. Classical electron micrographs of highly transcribed genes [such as ribosomal (rRNA) genes] look like Christmas trees, displaying strings of queuing ECs tightly packed on DNA (*13*, *14*). Here we tested a hypothesis that a cooperative effort by multiple RNAPs during transcription of the same DNA molecule ensures elongation to be extremely efficient. Using pure *E. coli* RNAP and various

Department of Biochemistry, New York University Medical Center, New York, NY 10016, USA.

*To whom correspondence should be addressed. E-mail: evgeny.nudler@med.nyu.edu